Optik - International Journal for Light and Electron Optics 241 (2021) 166203

Contents lists available at ScienceDirect

Optik

journal homepage: www.elsevier.com/locate/ijleo

Original research article

Effect of buffer nature, absorber layer thickness and temperature on the performance of CISSe based solar cells, using SCAPS-1D simulation program

M.A. Ghebouli [a,d,*], B. Ghebouli [b], R. Larbi [a], T. Chihi [c], M. Fatmi [d]

[a] Department of Chemistry, Faculty of Technology, University of Mohamed Boudiaf, M'sila, 28000, Algeria
[b] Laboratory of Studies Surfaces and Interfaces of Solids Materials, Department of Physics, Faculty of Sciences, University of Ferhat Abbas Setif 1, Setif 19000, Algeria
[c] Laboratory for Developing New Materials and their Characterization, Department of Physics, Faculty of Sciences, University of Ferhat Abbas Setif 1, 19000, Algeria
[d] Research Unit on Emerging Materials (RUEM), University of Ferhat Abbas Setif 1, 19000, Algeria

ARTICLE INFO

Keywords:
CISSe thickness layers
Zn_2SnO_4 buffer
SCAPS-1D

ABSTRACT

We report the performance of glass/Mo/CuInSSe(CISSe)/(Zn_2SnO_4, CdS, SnS_2)/ZnO thin films structures using solar cell capacitance simulator (SCAPS). Thin films solar cells with CuInSSe absorber layer reduce the cost and have comparable performance parameters with the conventional ones. The temperature effect on efficiency and fill factor is less noticeable in solar cell with Zn_2SnO_4 buffer layer. The average temperature gradient of CdS, SnS_2 and Zn_2SnO_4 based cells value is -0.317 %/K, -0.533 %/K and -0.539 %/K. An efficiency of 18.53 % has been achieved with Zn_2SnO_4 buffer for Voc, Jsc and FF of 0.5153 V, 45.4 $mAcm^{-2}$ and 79.17. The desired thickness of the CuInSSe (CISSe) absorber layer is estimated as 1.8 μm. The best performance obtained with Zn_2SnO_4 buffer can be explained by its higher transmission in the short wavelength range because its high gap 3.35 eV compared to those of CdS 2.4 eV and SnS_2 2.24 eV.

1. Introduction

Recently, there is considerable interest in renewable energy research in the field of photovoltaic technology. This is due to the development of new techniques for developing and improving the conversion efficiency of solar cells. Solar cells are costly because of the use of very expensive materials and processing techniques. The solution lies in the use of thin films based on semiconductors, which consume less material. The reduction of solar cells cost consists in the use of less expensive and non toxic materials [1–4]. These semiconductors must show adequate electronic and optical parameters such as the band gap, high emission quantum yield, the low turn on voltage and high efficiency energy conversion. New materials used in thin films solar cells have attracted researchers in order to achieve the desired efficiency at an acceptable cost. Solar cells based on chalcopyrite materials are distinguished by their absorbent layer, the thickness which does not exceed 2.5 μm and absorbs the useful part of the solar spectrum. Solar cells consisting of copper-based semiconductors having low band gap such as CIS, CGS, CIGS and CIGSS chalcopyrite show higher conversion efficiency among existing thin-film technologies [5]. These compounds suggest the benefits of a controllable band gap from 1 eV ($CuInSe_2$) to

* Corresponding author at: Department of Chemistry, Faculty of Technology, University of Mohamed Boudiaf, M'sila, 28000, Algeria.
E-mail address: mohamedamine.ghebouli@univ-msila.dz (M.A. Ghebouli).

https://doi.org/10.1016/j.ijleo.2020.166203
Received 14 July 2020; Received in revised form 26 November 2020; Accepted 18 December 2020
Available online 23 December 2020

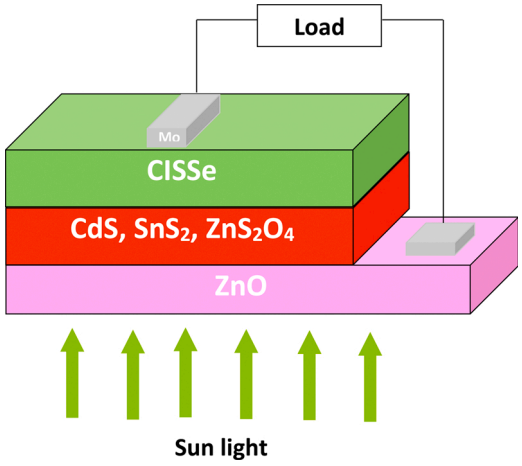

Fig. 1. The schematic diagram of solar cell structure.

Table 1
Physical parameters of CISSe, Zn_2SnO_4, CdS, SnS_2 and ZnO layers us ed in the simulation [14].

Material properties	CISSe	Zn_2SnO_4	CdS	SnS_2	ZnO
Thickness (μm)	Variable	0.1	0.1	0.1	0.2
Bandgap (E_g)	1.040	3.3500	2.4	2.2400	3.30
Electron affinity χ	4.300	4.5000	4.4	4.2400	4.500
Dielectric permittivity ε	12.000	9.000	10	10.000	9.000
CB density of state	1.000E + 19	2.200E + 18	2.2 E+18	2.200E + 18	2.200E + 18
VB density of state	1.000E + 19	1.800E + 19	1.8E+19	1.800E + 19	1.800E + 19
Electron thermal velocity	1.000E + 7	1.000E + 7	1E+7	1.000E + 7	1.000E + 7
Hole thermal velocity	1.000E + 7	1.000E + 7	1E+7	1.000E + 7	1.000E + 7
Electron mobility	1.000E + 2	3.200E + 1	1E+2	5.000E + 1	1.000E + 2
Hole mobility	2.500E + 1	3.000E + 0	2.500E + 1	5.000E + 1	2.500E + 1
Donor density	1.000E + 5	1.000E + 19	1E+18	1.000E + 17	1.000E + 18
Acceptor density	1.000E + 16	0.000E + 0	0	0.000E + 0	1.000E + 5
Absorption coefficient	Scaps value	Scaps value	Scaps value	Scaps value	Scaps value

2.43 eV ($CuGaS_2$) [6]. The understanding and design of solar cells based on crystalline, polycrystalline and amorphous materials have attracted a great interest in numerical simulation [7–10]. Among the published articles in the literature that are related to our work, we cite the impact of different absorbers and buffers. Saif Ahmed et al. offer a theoretical study of a solar cell structure Au/MoO3/C-s2TiBr6/SnO2/FTO with a Cs_2TiBr_6 perovskite absorber without lead, ecological and stable [11]. Solar cell structure glass/-Mo/$Cu_2ZnSnSe_4$/CdS/ZnO was studied by photoluminescence spectra [12]. The simulation of cadmium sulfide (CdS) and cadmium telluride (CdTe) based solar cell (Au/NiO/CdTe/CdS/ZnO/) has been presented [13]. F. Belarbi et al. evaluate the photovoltaic parameters for solar cells glass/Mo/CZTS/(CdS, SnS_2, Zn_2SnO_4)/ZnO as a function of the buffer layer thickness [14].

In our investigation, we use the structure of thin films solar cells, with CuInSSe (CISSe) as absorber layer. However, the difficulty lies in the number of parameters that influence the solar cells performance. ZTO (Zn_2SnO_4), CdS and SnS_2 are alternative buffers, while ZnO thin film is used as window. The aim of this work is to offer a CuInSSe (also known as CISSe) solar cell with high efficiency, using a suitable buffer layer. The solar cell structure consists of a glass plat substrate of thickness about 3 mm, on which is deposited a metal contact of molybdenum (Mo), then the CuInSSe absorber layer is deposited with thickness ranging from 0.2 to 3 μm. After that we insert the buffer layer such as (Zn_2SnO_4, CdS, SnS_2) and the ZnO window layer. Buffers are selected in such a way that they are non-toxic and show adequate electronic and optical properties (gap between 1 and 3.5 eV, higher absorption and transmission).We test with several buffers and we choose the ones that give the best efficiency. In the realization of the solar cell, the optimum thickness must not be exceeded, then we consume low expensive material and consequently the cost of the solar cell is reduced. We also choose materials that less cost. Obtaining the performance parameters of CISSe based solar cell (Short-circuit current density Jsc, open circuit voltage Voc, fill factor ff and efficiency η) required the use of a numerical analysis by SCAPS-1D. The solar cells structures investigated in this work are glass/Mo/CuInSSe(CISSe)/(Zn_2SnO_4, CdS, SnS_2)/ZnO.

2. Simulation procedure

Fig. 1 shows a standard schematic diagram of the solar cell structure investigated in this work with its constituents glass/Mo/(CISSe)/(Zn_2SnO_4, CdS, SnS_2)/ZnO. The approach to achieve adequate efficiency is the use of numerical simulation to explore the general solar cell characteristics and its performance. Table 1 reports the physical parameters of solar cell used in the simulation. The

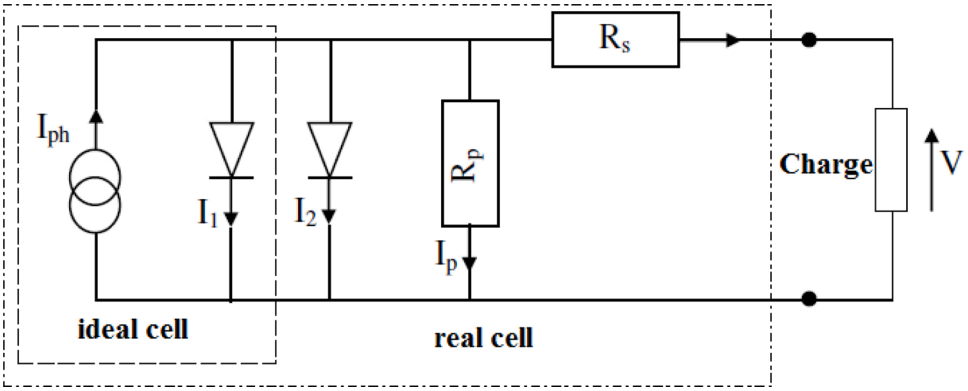

Fig. 2. The model of solar cell structure with series and parallel resistances.

structure is studied under AM 1.5 solar spectrum, the power of incident light being P = 1000 W.m^{-2} and ambient temperature T =300 K. We report the obtained results, specifying the parameters that we vary, as well as the values of the parameters that are kept constant. The optimized parameters (back contact, CISSe buffer layer, window layer and metallic protective layer) were taken from literature.

2.1. Study as a function of CuInSSe (CISSe) absorber layer thickness

ZnO, (Zn_2SnO_4, CdS, SnS_2) layer thicknesses are set respectively to 0.2 and 0.1 μm. The temperature is maintained constant 300 K. The series resistance is taken to be zero with an infinitely shunt resistance. The CuInSSe (CISSe) thin film thickness varies between 0.2 and 3 μm.

2.2. Study as a function of temperature

ZnO, (Zn_2SnO_4, CdS, SnS_2) and CuInSSe (CISSe) layers thicknesses are set to 0.2, 0.1 and 1.8 μm. The series resistance is taken to be zero with an infinitely shunt resistance. The temperature varies in the range 272–312 K.

2.3. Study as a function of buffer nature

Three buffers Zn_2SnO_4, CdS and SnS_2 are used intermittently. The buffer, the window and the CuInSSe (CISSe) absorber layers thicknesses are set 0.1, 0.2 and 2 μm. The temperature is maintained constant 300 K. The series resistance is taken to be zero with an infinitely shunt resistance.

2.4. Study as a function of series resistance

ZnO, (Zn_2SnO_4, CdS, SnS_2) and CuInSSe (CISSe) layers thicknesses are set to 0.2, 0.1 and 1.8 μm. The temperature is maintained constant 300 K. The series resistance varies from 0–4 Ω cm^2. The calculation of the current actually delivered to the charge of the circuit taking into account the limits of the solar cell requires the introduction of an electrical circuit composed of a current source, two diodes and a parallel resistance to another series. This model which represents the equivalent circuit diagram of the solar cells is reported in Fig. 2. The leakage current in the solar cell is modeled by a parallel resistance R_p. The leakage current enters between the edges of the cell or through the transmitter. The parallel resistance R_p must be quite high. The series resistance Rs translates the resistive losses in the solar cell (base and emitter), in the metal/semiconductor interface and in the metal itself. The minimization of its negative influence on the solar cell requires the use of series resistance quite low.

3. Simulation program and material parameters

Solar Cell Capacitance Simulator (SCAPS-1D) is a digital simulation software dimensional solar cell developed at the Department of Electronics and Information Systems IT (ELIS), University of Gent, Belgium, and it is used for the numerical analysis of solar cells [15, 16]. This software is free and available for photovoltaic research community. It runs on PC operating systems Windows 95, 98, NT, 2000, XP, Vista, Windows 7, Windows 8 and takes on about 50 MB spaces on the disc. SCAPS was originally developed for the family of $CuInSe_2$ and CdTe cell structures. The model is based on solving the Poisson's equation which connects the charge to the electrostatic potential and hole-continuity equations. SCAPS program allows one to simulate structures consisting of a defined number of layers (up to 7 intermediate layers), excluding front and back contacts. The realization of this paper requires the use of the numerical simulation of the solar cell CuInSSe (also known CISSe) absorber using a SCAPS-1D version 3.3.07. We investigated the effect of CuInSSe (CISSe) layer thickness, the temperature, the buffer layer nature and the series resistance on the parameters of solar cells Glass plate/Mo/

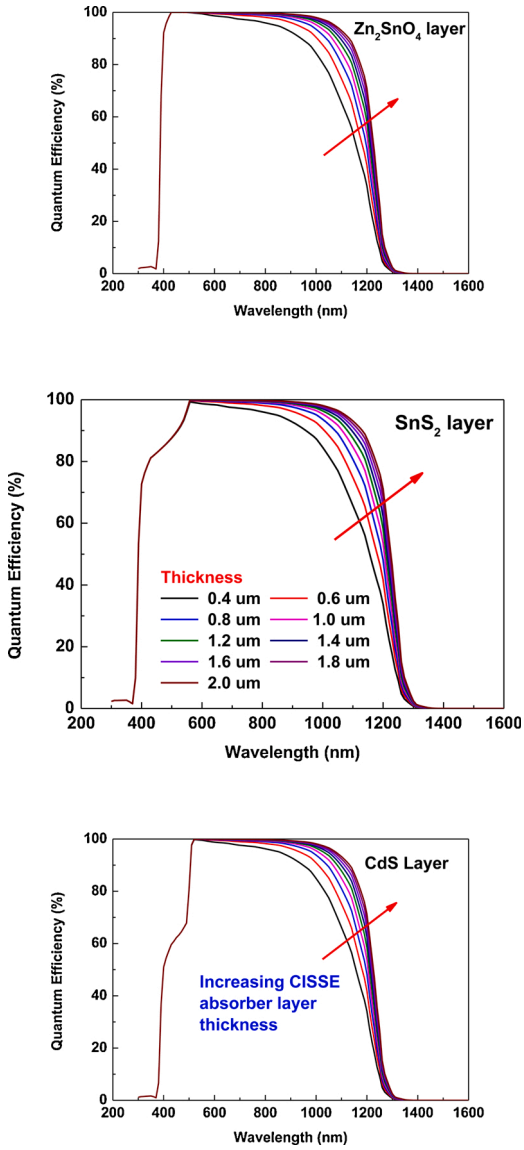

Fig. 3. The quantum efficiency (QE) of the solar cell structure CISSe/(Zn2SnO4, SnS_2, CdS).

CuInSSe (CISSe)/(Zn_2SnO_4, CdS, SnS_2)/ZnO.

4. Results and discussions

4.1. Effect of CuInSSe (CISSe) layer thickness and nature buffer

We fixe (Zn_2SnO_4, CdS, SnS_2) buffer and ZnO window layers thicknesses at 0.1 and 0.2 μm for the first step of simulation. The temperature is kept constant 300 K. The series resistance is taken to be zero. The quantum efficiency (QE) of the solar cell glass/Mo/(CISSe)/(Zn_2SnO_4, CdS, SnS_2)/ZnO as a function of the wavelength is illustrated in Fig. 3, whose thickness of the CISSe layer varies from 0.4 μm to 1.8 μm with a step of 0.2 μm. With a decrease of the CISSe layer thickness, QE decreases for wavelength values ranging from 400 to 1300 nm. It produces insufficient absorption of photons in the case of CISSe thin film absorber [17]. The short-circuit current density (Jsc) and open circuit voltage (Voc) solar cell parameters as a function of CISSe layer thickness ranging from 0.2–3 μm and for various buffers are shown in Fig. 4. The first finding is that the short circuit current and open circuit voltage increase rapidly to a stagnation value. For thicker thin films solar cells, the CISSe active layer will absorb more photons and generate more electron-hole pairs [18]. From the obtained results, we conclude that the absorber layer thickness is an important factor for the absorption of photons [19]. According to Fig. 4, the optimum value of CISSe absorber thickness corresponds to a rapid increase in short circuit current. The optimum thickness of the absorber is 1.8 μm. When the thickness of the active layer increases from 0.2 to 1.8 μm,

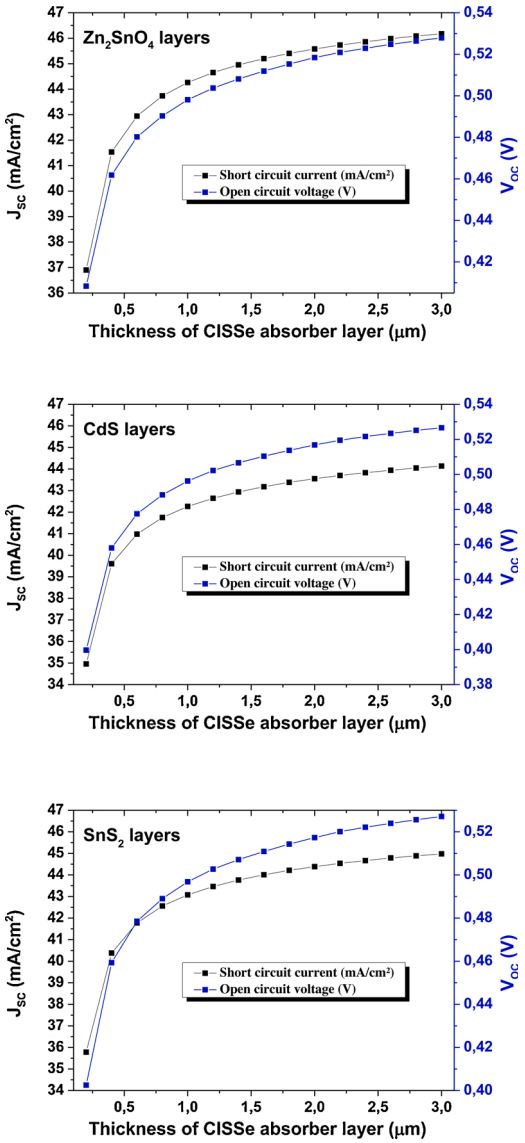

Fig. 4. Effect of CISSe thickness layer on short circuit current and open circuit voltage for solar cells (a) Zn_2SnO_4, (b) CdS, (c) SnS_2.

the short circuit current density increases considerably from 36.9 to 45.4 mA.cm^{-2}, 35.78 to 44.21 mA.cm^{-2} and 34.95 to 43.38 mA.cm^{-2} for the buffer layer Zn_2SnO_4, CdS and SnS_2 respectively. While, the open circuit voltage is enhanced from 0.408 to 0.515 V, 0.402 to 0.514 V and 0.399 to 0.513 V for Zn_2SnO_4, CdS and SnS_2 buffer layers. It is noted that the open circuit voltage is practically identical for the three buffers at optimum thickness and therefore the short circuit current is responsible in the performance of these solar cells. The efficiency and fill factor of the studied solar cells as a function of CISSe layer thickness for various buffers are visualized in Fig. 5. The increase in short circuit current and open circuit voltage bring with it the increase of the efficiency and fill factor. The efficiency (fill factor) calculated at optimum thickness is 18.53, 17.65 and 17.99 % (79.17, 79.19 and 79.1 %) for Zn_2SnO_4, CdS and SnS_2 buffers respectively. The efficiency (fill factor) calculated at thickness of 0.3 µm is 19.43, 18.51 and 18.87 % (79.69, 79.66 and 79.57 %) for Zn_2SnO_4, CdS and SnS_2 buffers respectively. The optimized performance parameters of solar cells (short circuit current density, open circuit voltage, efficiency and fill factor) achieved from the optimized glass/Mo/(CISSe)/(Zn_2SnO_4, CdS, SnS_2)/ZnO solar cells were taken from literature. The parameters that characterize a solar cell with various absorber and buffer layers cited by others researchers [11,13,14,19–21] are reported in Table 2. The conclusion drawn from these results is that our performance cells are vastly better except those cited in references [13,20]. Among the three buffers used in this work, the cell including Zn_2SnO_4 buffer layer gives the best efficiency. Fig. 6 shows the energy band diagram of glass/Mo/(CISSe)/(Zn_2SnO_4, CdS, SnS_2)/ZnO solar cells. Table 3 reports the energy levels of valence band E_v, conduction band E_c donor E_p and acceptor E_n. One remarks that the valence band offset (VBO) is negative for all buffers, consequently there has no barrier to flow photo-generated hole toward the back electrode. The J(V) characteristic for glass/Mo/(CISSe)/(Zn_2SnO_4, CdS, SnS_2)/ZnO solar cells is depicted in Fig. 7. The current density is reported to be

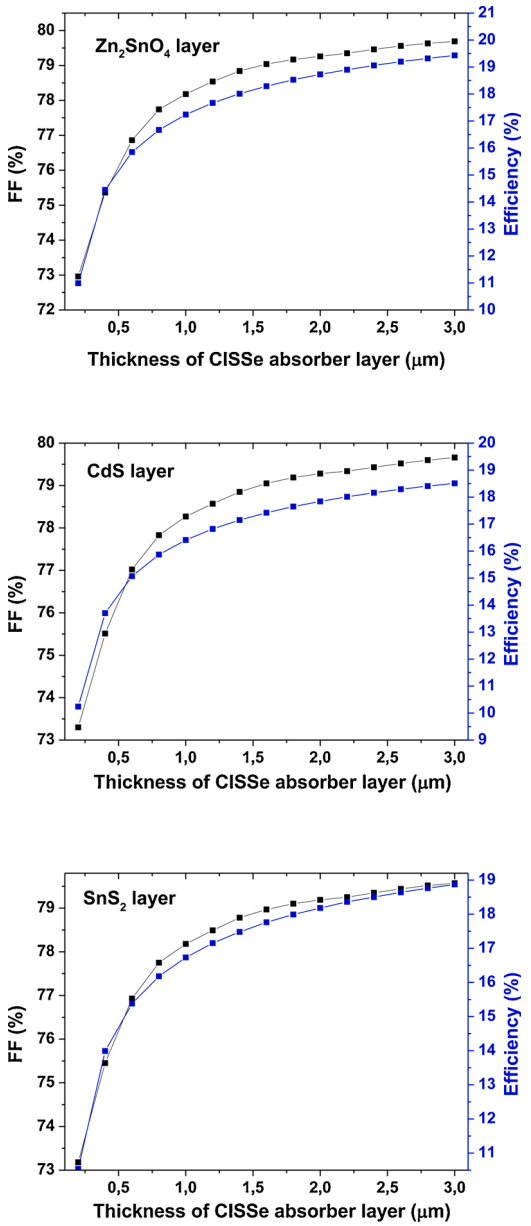

Fig. 5. Effect of CISSe thickness layer on efficiency and fill factor on solar cells (a) Zn_2SnO_4, (b) CdS, (c) SnS_2.

Table 2
The parameters that characterize a solar cell.

	Jsc (mA/cm^2)	Voc (V)	FF (%)	PCE (%)	Ref.
glass/Mo/(CISSe)/(CdS)/ZnO (sim)	43.38	0.5137	79.19	17.65	[TW]
glass/Mo/(CISSe)/(SnS_2)/ZnO (sim)	44.21	0.5143	79.1	17.99	[TW]
glass/Mo/(CISSe)/(Zn_2SnO_4)/ZnO (sim)	45.4	0.5153	79.17	18.53	[TW]
Au/P3HT/Cs_2TiBr_6/TiO_2/FTO (exp)	3.87	0.89	59.5	2.15	[19]
Au/P3HT/Cs_2TiBr_6/TiO_2/FTO (sim)	4.35	0.93	59.54	2.41	[11]
MoS_2/CZTS/CdS/ ZnO (sim)	24.98	0.7159	66.58	11.91	[14]
MoS_2/CZTS/SnS_2/ZnO (sim)	26.99	0.7178	65.67	12.73	[14]
MoS2/CZTS/ZTO/ZnO (sim)	24.93	0.7157	66.62	11.89	[14]
Au/MoO_3/ Cs_2TiBr_6/ SnO_2/FTO (sim)	8.66	1.53	86.45	11.49	[11]
Mo/CIGS/CZTSe/CdS/ZnO (sim)	43.7	0.6036	82.78	21.84	[20]
Au/NiO/CdTe/CdS/ZnO (sim)	29.1	1.0972	88.15	25.4	[13]

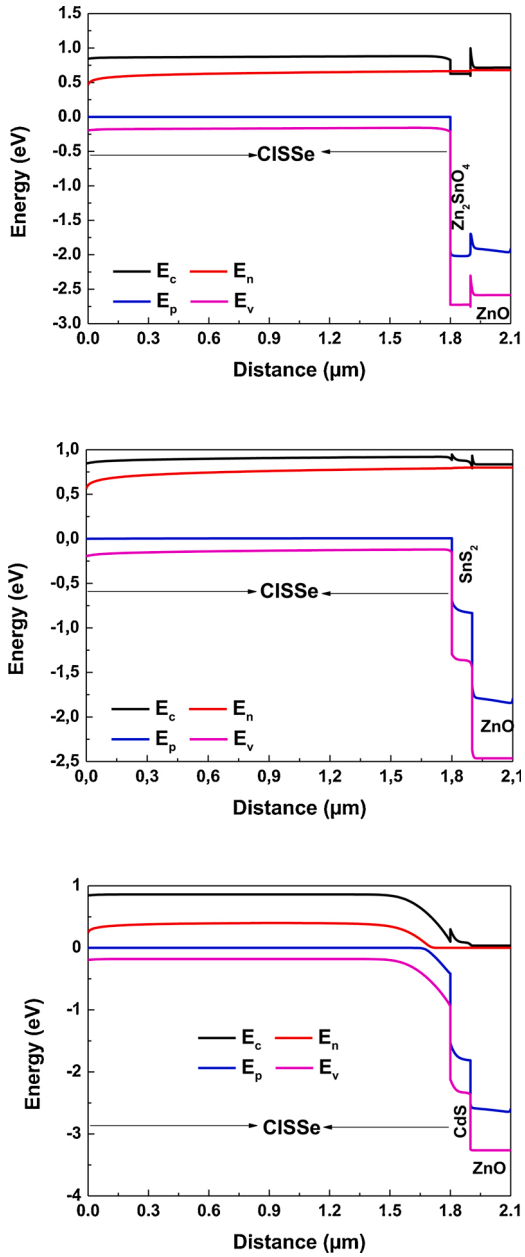

Fig. 6. Energy band diagram of the glass/Mo/(CISSe)/(Zn_2SnO_4, CdS, SnS_2)/ZnO.

Table 3
Energy levels of valence band E_v, conduction band E_c donor E_p and acceptor E_n for Zn_2SnO_4, CdS and SnS_2 buffers.

	Zn_2SnO_4	CdS	SnS_2
E_c (eV)	0.8271	0.2995	0.9147
E_n (eV)	0.663	5.4×10^{-5}	0.2282
E_p (eV)	−2.0005	−1.6204	−1.747
E_v (eV)	−2.7251	−2.174	−1.3227

increasing according to the sequence $Zn_2SnO_4 \rightarrow SnS_2 \rightarrow$ CdS. The increase in current density becomes rapidly from the voltage of 0.38 V, where its value is -42.61, -43.39 and -44.62 mA. cm^{-2} for CdS, SnS_2 and Zn_2SnO_4. It reaches the value -17.65, -17.48 and -19.85 mA. cm^{-2} for CdS, SnS_2 and Zn_2SnO_4 at a voltage of 0.5 V.

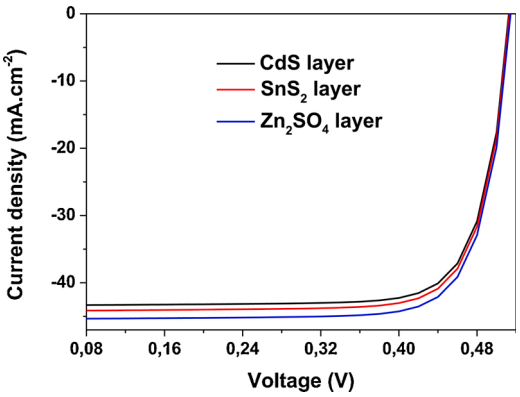

Fig. 7. J(V) characteristic for glass/Mo/(CISSe)/(Zn_2SnO_4, CdS, SnS_2)/ZnO solar cells.

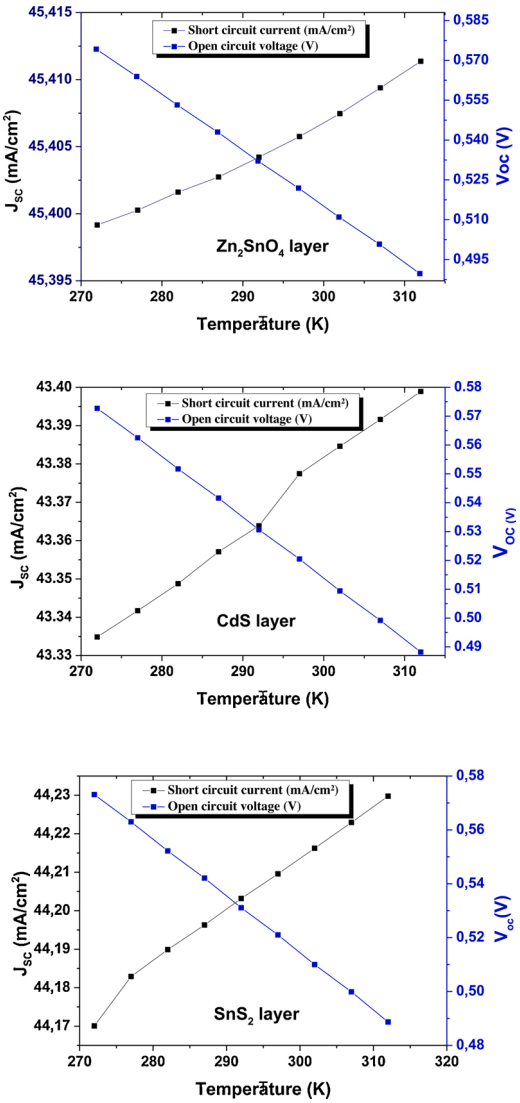

Fig. 8. The temperature effect on short circuit current and open circuit voltage for solar cells (a) Zn $_2SnO_4$, (b) CdS, (c) SnS_2.

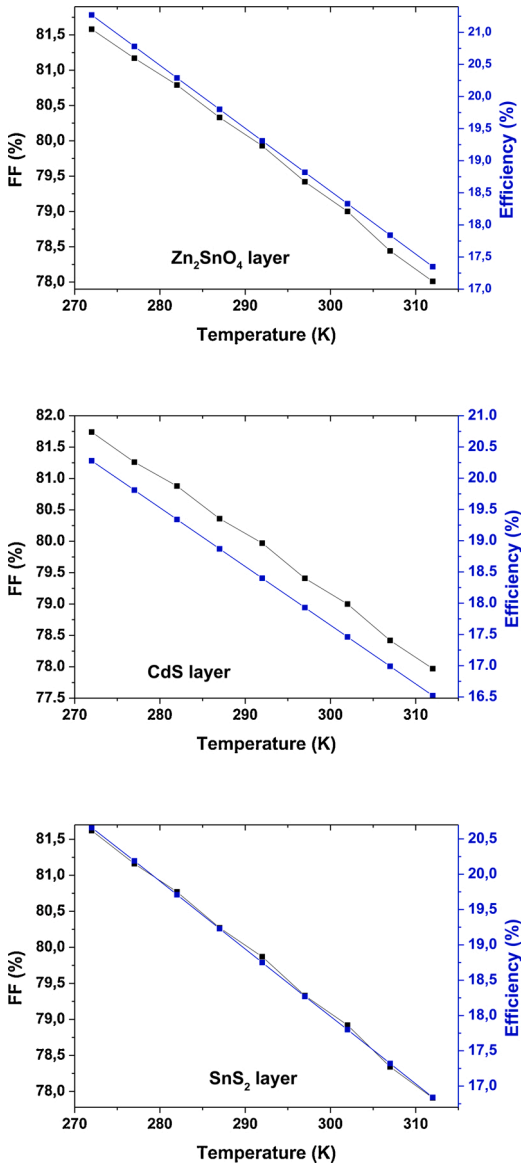

Fig. 9. The temperature effect on efficiency and fill factor for solar cells (a) Zn_2SnO_4, (b) CdS, (c) SnS_2.

4.2. *Effect of temperature on solar cells parameters*

We fix ZnO layer window, (Zn_2SnO_4, CdS, SnS_2) buffer layer and CISSe absorber layer thicknesses at 0.2, 0.1 and 1.8 μm. The series resistance is taken to be zero. We vary the temperature in the range 272–312 K. The saturation current in the dark and in the spatial load zone are proportional to the square of the intrinsic concentration ni^2 [22,23]. An increase in intrinsic concentration increases the saturation current density and leads to a decrease in open circuit voltage (Voc). By observing Fig. 8, one can see that the increase in temperature leads to a decrease in the open circuit voltage (Voc) and an increase in short circuit current density (Jsc). When the temperature changes from 272 to 312 K, one remarks that the decrease in voltage is more important than the increase in current density. Therefore, the maximum solar cell power decay. Consequently, the temperature has a detrimental effect on solar cell parameters. Fig. 9 shows the temperature effect on efficiency (η) and fill factor (ff) parameters of studied solar cells. It can be seen that efficiency (fill factor) decreases linearly with increasing temperature in the range 272–312 K. In this temperature range, the increase (decrease) in short circuit current density (open circuit voltage) is 0.0122, 0.0641 and 0.186 $mA.cm^{-2}$ (0.0845, 0.0845 and 0.0016 V) for Zn_2SnO_4, CdS and SnS_2 buffers. These results reflect a decrease in power of 0.01, 0.054 and 0.002 $W.m^{-2}$ for Zn_2SnO_4, SnS_2 and CdS buffer. Therefore, the temperature effect on efficiency and fill factor is less noticeable in CdS buffer layer case. The effect of working temperature on the performance of glass/Mo/(CISSe)/(Zn_2SnO_4, CdS, SnS_2)/ZnO solar cells has been investigated by changing operating temperature from 300 K to 330 K. The normalized efficiency for Zn_2SnO_4, CdS, SnS_2 and without buffer based cells decreases

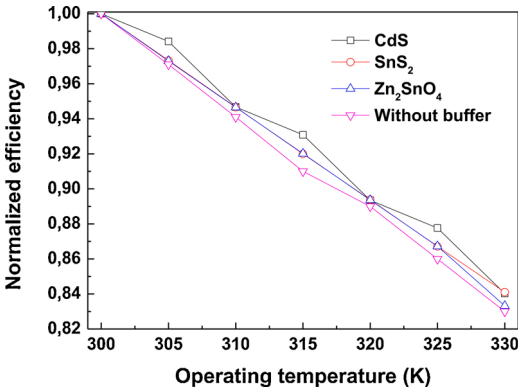

Fig. 10. Temperature gradient of CISSe cells with CdS, SnS_2 and Zn_2SnO_4 and without buffer layer.

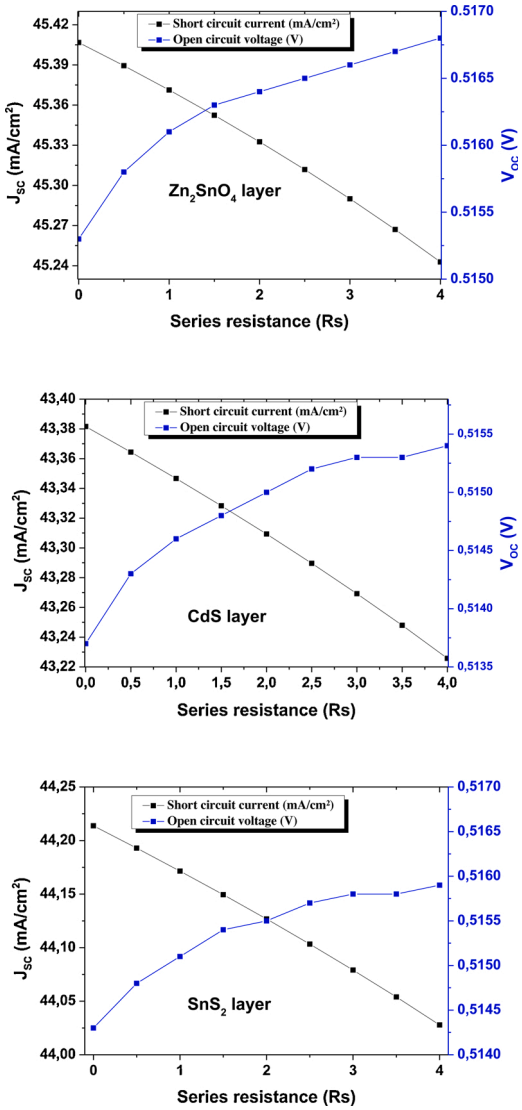

Fig. 11. The series resistance effect on short circuit current and open circuit voltage for solar cells (a) Zn_2SnO_4, (b) CdS, (c) SnS_2.

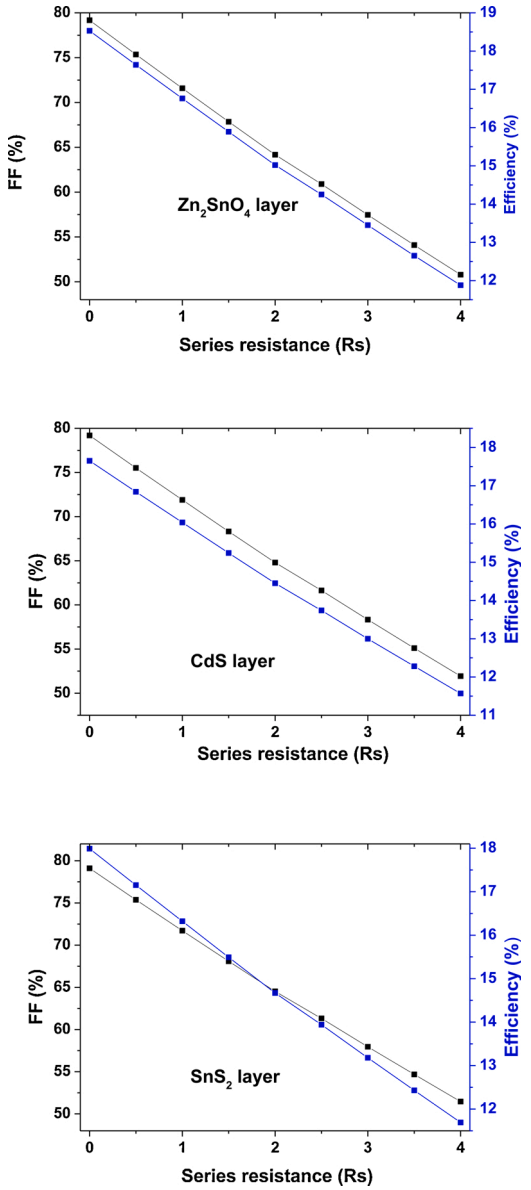

Fig. 12. The series resistance effect on efficiency and fill factor for solar cells (a) Zn_2SnO_4, (b) CdS, (c) SnS_2.

when the operating temperature enhanced, with average temperature coefficient value of -0.539 %/K, -0.317 %/K, -0.533 %/K and -0.58 %/K as shown in Fig. 10. This result confirms that temperature more affects the performance of the solar cell following the sequence CdS→SnS_2→Zn_2SnO_4→without buffer. The effect of the temperature gradient on solar cell performance is greater in the absence of buffer.

4.3. Effect of series resistance on solar cells parameters

We fixe (Zn_2SnO_4, CdS, SnS_2) buffer layer, ZnO window layer and CISSe layer thicknesses at 0.1, 0.2 and 1.8 μm. The temperature is taken to be 300 K. The series resistance varies in the range 0–4 Ω cm^2. We present the series resistance effect on short-circuit current density (J_{sc}) and open circuit voltage (V_{oc}) in Fig. 11. The open circuit voltage (short-circuit current density) increases (decreases) linearly when the series resistance is enhanced. In this range of series resistance, the increase (decrease) in short circuit current density (open circuit voltage) is 0.11, 0.14 and 0.11 (0.002, 0.001 and 0.002) for buffer layer Zn_2SnO_4, Sn_2S and CdS. When the series resistance varies from 0–4 Ω cm^2, one remarks that the increase in short circuit current density is more important than the decrease in open circuit voltage. Therefore, there is a reduction of 0.0022, 0.0014 and 0.0022 $W.m^{-2}$ in solar cell power formed with Zn_2SnO_4, SnS_2 and CdS buffer layer. Consequently, the negative effect of series resistance on studied solar cells is more significant in the buffer

layer Zn_2SnO_4 case. Fig. 12 visualizes the effect of series resistance on efficiency and fill factor of solar cell. The efficiency (fill factor) decreases from 18.53 (79.17), 17.65 (79.19) and 17.99 (79.1) to 11.88 (50.79), 11.57 (51.93) and 11.69 (51.47) when the series resistance increases in the range 0–4 Ω cm^2 for Zn_2SnO_4, SnS_2 and CdS buffers. When the series resistance is enhanced from 0–4 Ω cm^2, there is a reduction in efficiency (fill factor) of 6.65, 6.08 and 6.3 % (28.38, 27.26 and 27.63 %) for buffer layer Zn_2SnO_4, CdS and Sn_2S. It can be seen that the series resistance have an important negative effect on the degradation of the solar cell performance in all studied buffers.

5. Conclusion

We performed numerical simulation for CuInSSe (CISSe) solar cell using Zn_2SnO_4, CdS and SnS_2 buffer layers. Solar cell parameters were reported by varying buffer layer nature, CuInSSe absorber layer thickness, temperature and series resistance. Among all kinds of buffer layers studied, cell with Zn_2SnO_4 buffer layer revealed the best efficiency of 18.53 %. The results show that the solar cell performances are affected by the increase in operating temperature for all buffer layers with differences in temperature gradients. The photovoltaic parameters (Jsc, η, Voc and FF) have been investigated in this simulation study. The temperature more affects the performance of the solar cell buffer-based following the buffer sequence CdS→ SnS_2→ Zn_2SnO_4. We were able to obtain an efficiency, which can be further increased by optimizing other parameters of the cell, such as the gap and the doping density of different layers. The valence band offset is negative, and then there has no barrier to flow photo-generated hole toward the back electrode. The effect of the temperature gradient on solar cell performance is greater in the absence of buffer.

Declaration of Competing Interest

The authors report no declarations of interest.

References

[1] X.X. Wu, High-efficiency polycrystalline CdTe thin-film solar cells, Sol. Energy 77 (2004) 803–814.
[2] P. Jackson, D. Hariskos, E. Lotter, S. Paetel, R. Wuerz, R. Menner, W. Wischmann, M. Powalla, New world record efficiency for Cu(In,Ga)Se2 thin-film solar cells beyond 20%, Prog. Photovoltaics Res. Appl. 19 (2011) 894–897.
[3] M.M.A. Green, Photovoltaics energy payback times, greenhouse gas emissions and external costs, Prog. Photovolt. Res. Appl. 14 (2006) 275–280, https://doi.org/10.1002/pip.706.
[4] B.A. Anderson, C. Azar, J. Holmberg, S. Karlsson, Material constraints for thin-film solar cells, Energy 23 (1998) 407–411.
[5] M.A. Green, K. Emery, Y. Hishikawa, W. Warta, Solar cell efficiency table (version37), Prog. Photovolt. Res. Appl. 19 (2011) 84–92.
[6] J. Kaneshiro, N. Gaillard, R. Rocheleau, E. Miller, Advances in copper-chalcopyrite thin films for solar energy conversion, Sol. Energy Mater. Sol. Cells 94 (2010) 12–16.
[7] A. Morales-Acevedo, N. Hern_andez-Como, G. Casados-Cruz, Modeling solar cells: a method for improving their efficiency, Mater. Sci. Eng. B 177 (2012) 1430–1435.
[8] A. Aissat, M. El beya, R. Bestam, J.P. Vilcot, Modeling and simulation of $Al_xGa_yIn_{1-x-y}As$/InP quaternary structure for photovoltaic, Int. J. Hydrogen Energy 39 (2014) 15287–15291.
[9] Wang Dong Lin, Cui HuiJuan, Su Gang, Modeling method to enhance the conversion efficiency by optimizing light trapping structure in thin-film solar cells, Sol. Energy 120 (2015) 505–513.
[10] H. Arbouz, A. Aissat, J.P. Vilcot, Modeling and optimization of CdS/$CuIn_{(1-x)}Ga_xSe_2$ structure for solar cells applications, Int. J. Hydrogen Energy 41 (2016) 20987–20992.
[11] Saif Ahmed, Farihatun Jannat, Md. Abdul Kaium Khan, Mohammad Abdul Alim, Numerical development of eco-friendly Cs_2TiBr_6 based perovskite solar cell with all-inorganic charge transport materials via SCAPS-1D, Optik (2020).
[12] M.A. Sulimov, M.N. Sarychev, M.V. Yakushev, J. Márquez-Prieto, I. Forbes, V.Yu Ivanov, P.R. Edwards, A.V. Mudryi, J. Krustok, R.W. Martin, Effects of Irradiation of ZnO/CdS/Cu2ZnSnSe4/Mo/glass Solar Cells by 10 MeV Electrons on Photoluminescence Spectra, Materials Science in Semiconductor Processing, 121, 2021, p. 105301.
[13] Shamim Ahmmed, Asma Aktar, Md. Ferdous Rahman, Jaker Hossain, Abu Bakar Md. Ismail, A numerical simulation of high efficiency CdS/CdTe based solar cell using NiO HTL and ZnO TCO, Opt. – Int. J. Light Electron. Opt. 223 (2020), 165625.
[14] F. Belarbi, W. Rahal, D. Rached, S. Benghabrit, M. Adnane, A comparative study of different buffer layers for CZTS solar cell using Scaps-1D simulation program, Opt. – Int. J. Light Electron. Opt. 216 (2020), 164743.
[15] Marc Burgelman, Koen Decock, Alex Niemegeers, Johan Verschraegen, Stefaan Degrave, SCAPS Manual, 2019. February (Book).
[16] M. Burgelmann, P. Nollet, S. Degrave, Modelling polycrystalline semiconductor solar cells, Thin Solid Films 361–362 (2000) 527–532.
[17] N. Amin, K. Sopian, M. Konagai, Numerical modeling of CdS /CdTe and CdS /CdTe/ZnTe solar cells as a function of CdTe thickness, Sol. Energy Mater. Sol. Cells 91 (2007) 1202–1208.
[18] P. Chelvanathan, M.I. Hossain, N. Amin, Thickness optimisation of various layers CZTS solar cell, App. Phys. 10 (2010) 5387–5391.
[19] M. Patel, A. Ray, Enhancement of output performance of Cu_2ZnSnS_4 thin film solar cells a numerical simulation approach and comparison to experiments, Phys. B 407 (2012) 4391–4397.
[20] Min Chen, Ju Ming-Gang, Alexander D. Carl, Yingxia Zong, Ronald L. Grimm, Gu Jiajun, Xiao Cheng Zeng, Yuanyuan Zhou, Nitin P. Padture, Cesium titanium (IV) bromide thin films based stable lead-free perovskite solar cells, Joule 2 (3) (2018) 558–570, https://doi.org/10.1016/j.joule.2018.01.009.
[21] H. Heriche, I. Bouchama, N. Bouarissa, Z. Rouabah, A. Dilmi, Enhanced efficiency of Cu(In,Ga)Se_2 solar cells by adding $Cu_2ZnSn(S,Se)_4$ absorber layer, Opt. – Int. J. Light Electron. Opt. 144 (September) (2017) 378–386.
[22] A. Luque, S. Hegedus, Handbook Photovoltaic Science and Engineering, John Wiley & Sons Ltd, Chichester, 2003, https://doi.org/10.1002/0470014008. ISBN: 0-471-49196-49199.
[23] T. Markvart, Luis Castaner, Practical Handbook of Photovoltaic: Fundamentals and Applications, Elsevier Ltd., 2003.